J Mater Sci (2007) 42:6161–6170
DOI 10.1007/s10853-006-1164-7

A novel nozzle design for producing hydroentangled nonwoven materials with minimum jet-mark defects

Nagendra Anantharamaiah · Katharina Römpert · Hooman Vahedi Tafreshi · Behnam Pourdeyhimi

Received: 26 July 2006 / Accepted: 18 October 2006 / Published online: 17 April 2007

Abstract The presence of jet-marks, or jet-streaks, on the surface of hydroentangled nonwoven fabrics, is usually regarded as an undesirable outcome of the hydroentangling process. Jet-streaks degrade aesthetic features and physical properties of the resulting fabrics. Jet-streaks are associated with low tear strength along the machine direction and non-uniform appearance. Reducing or eliminating the occurrence of jet-streaks will lead to increased use of this class of fabrics in many applications. Hydroentangling employs closely-packed single or multiple rows of high-speed waterjets to entangle and consolidate fibers or filaments in a loose (un-bonded) web. In this work, we demonstrated that a waterjet curtain made of two rows of staggered jets where the jets in the 2nd row are smaller in diameter than those in the 1st row can help minimize these jet-marks in a cost-effective manner. The optimal ratio between the diameter of the jets in the 1st and 2nd row depends on the hydroentangling pressure, as well as the web characteristics. In this study, different nozzle diameters ranging from 100 μm to 130 μm for the 2nd row were examined in combination with a fixed diameter of 130 μm for the nozzles in the 1st row. For the type of fiber-web used and the operating pressures considered, a combination of nozzles with 130 μm diameter in the 1st row, and nozzles with 110 μm diameter in the 2nd row, was found to provide the optimum setting for eliminating/minimizing the jet-marks.

N. Anantharamaiah · K. Römpert · H. Vahedi Tafreshi (✉) · B. Pourdeyhimi
Nonwovens Cooperative Research Center, North Carolina State University, Raleigh, NC 27695-8301, USA
e-mail: hvtafres@ncsu.edu

K. Römpert
Freudenberg Forschungsdienste, 69465 Weinheim, Germany

Introduction

Nonwoven materials, by definition, are assemblies of fibers bonded together in the form of sheets, webs, or mats [1]. Nonwovens are used in the areas of filtration, composites, geotextiles, hygiene and medical products, as well as clothing and protective garments, amongst many others. Nonwovens are bonded mechanically, thermally or chemically. Hydroentangling is a mechanical bonding process and most popular because the resulting fabric is strong, flexible and most fabric-like [2, 3]. The underlying mechanism in hydroentanglement is the exposure of the fibers to a non-uniform spatial pressure field created by a successive bank of closely-packed high-speed waterjets. The impact of the waterjets with the fibers in a somewhat random web displaces and rotates them with respect to their neighbors. During these relative displacements, some of the fibers twist around others and/or interlock with them [4–8]. The final outcome is a compressed and strong sheet of entangled fibers.

Hydroentangling waterjets are generated from tiny cone-capillary nozzles with a typical inlet diameter of about 130 μm (see Fig. 1). Hydroentangling nozzles are normally placed on long stainless steel strips, normally referred to as ''nozzle-strips''. Nozzle-strips span across the width of the machine (often a few meters). The nozzle-to-nozzle distance (spacing between waterjets) is usually about 500–600 μm. Each nozzle-strip is normally placed in a manifold (jet head) where high-pressure water is supplied to the nozzles. The generated waterjets are collimated streams with glassy appearance and impact the web. Hydroentangling machines normally have several manifolds. Often, entanglement is accomplished by pre-bonding the web at lower pressures and then entangling the web at higher pressures using the manifolds further downstream. A schematic illustration of the hydroentangling machine used in this study is shown in

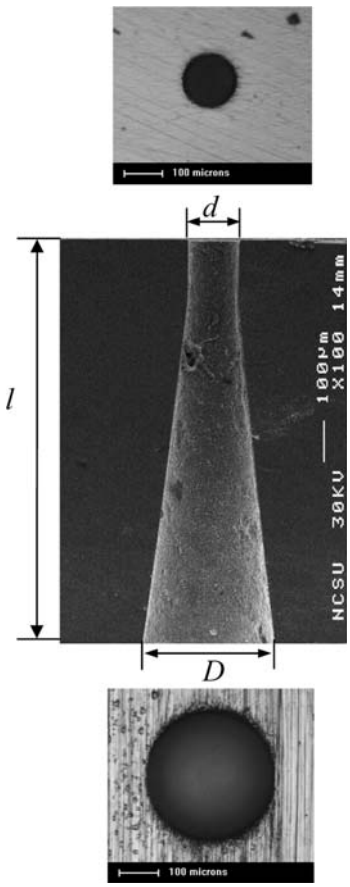

Fig. 1 SEM image of a typical hydroentangling nozzle with an inlet diameter of 130 µm

Fig. 2. Note that as long as the jet maintains its characteristics and does not breakup, higher manifold pressures will translate to greater impact energy [9].

Different kinds of fiber-webs can be bonded by hydroentangling. These webs can be made of long fibers (continuous filaments), as in spun-bonded webs, or discontinuous fibers, like the webs produced via carding, air-laying, and wet-laying processes. Alternatively, a combination of webs made of short and long fibers can also be hydroentangled together to make a composite structure depending on the desired end-use. The stand-off distance of the fiber-web from the nozzle exit is normally less than 5 cm. The webs are carried by a moving belt or a rotating perforated drum (also called a forming surface). There is one vacuum box for each manifold, underneath the belt, and/or inside the drum, which extract the water from the web for efficient entanglement.

The impact of the waterjets with the web displaces the fibers forming the so-called jet-marks, or jet-streaks on the fabric surface (see Fig. 3). Jet-streaks are undesirable in applications where aesthetics and structural integrity of the fabric are important. The jet streaks cause ridges that are clearly visible. These ridges also cause density variations locally and lead to local variations in mechanical properties. Hydroentangled fabrics often have low tear strength in the machine direction or along the jet-streaks. Similarly, when a tear propagates in the cross direction, the path changes and follows the jet-streaks. Hydroentangling at low pressures often leads to relatively more isotropic tear properties because the jet-streaks are not as pronounced. However, high pressures are often needed to achieve good fiber entanglement.

There have been several attempts in the past to remove or reduce jet-streaks. One of the methods explored introduced oscillations of the manifolds in the transverse direction (perpendicular to the fabrics' direction of travel) which in turn led to oscillations in the waterjet curtain [10]. The movement was regulated by connecting the manifold to a reciprocating unit (such as a vibrator). This method obviously requires a major capital investment as well as an additional source of energy for vibrating the manifolds. Nevertheless, the final outcome of such a technique is to transform the linear streaks into zigzag pattern without completely eliminating them. Another method relied on 4-row nozzle-strips having nozzles with the same diameter in a staggered arrangement [11]. This method does not eliminate the jet-streaks because all the nozzles have

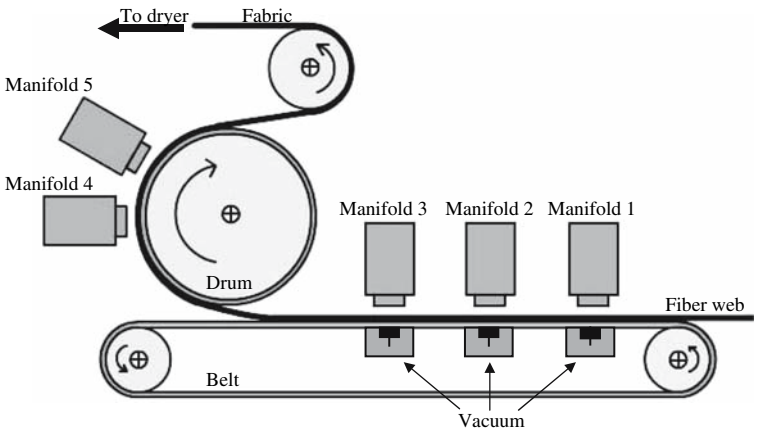

Fig. 2 Schematic of a typical hydroentangling unit

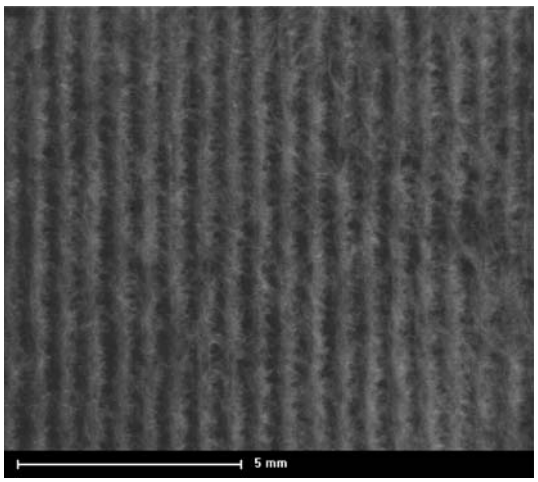

Fig. 3 A hydroentangled fabric having visible jet streaks on its surface

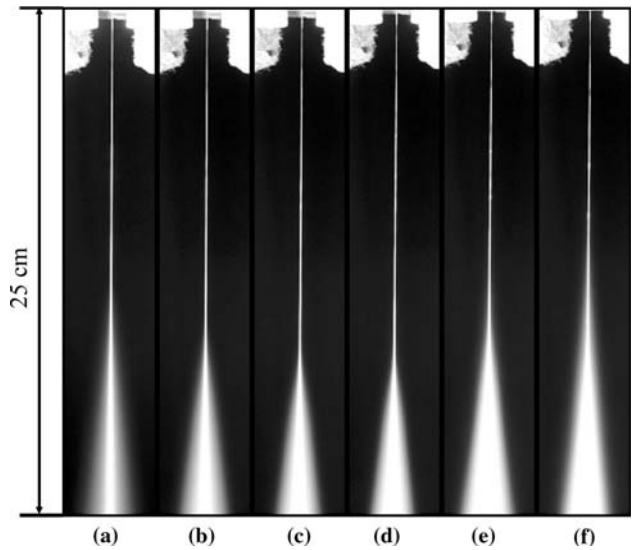

Fig. 4 Profiles of the waterjets generated via a typical hydroentangling nozzle with a diameter of 130 μm at different pressures (**a**) 35 bars, (**b**) 70 bars, (**c**) 100 bars, (**d**) 135 bars, (**e**) 170 bars, and (**f**) 200 bars

identical diameters, and the resulting waterjets have the same impact energy and the jet-streaks caused by the last row of nozzles will permanently stay on the fabric.

Other attempts include the work of Oathout et al. [12], who discharged the waterjets with two opposite offset angles (towards the sides of the fabric) with respect to the vertical direction, the work of Zolin, who designed a system where the fabric moved on a series of rotating drums, with manifolds placed at different angles with respect to the fabric [13], and the work by Greenway et al., who moved the fabric transversely over a drum, combined with oscillating manifolds [14]. However, their designs were either inefficient or too expensive to be used in general commercial applications.

In this paper, we report on our experimental study aimed at minimizing the jet-streaks in hydroentangled fabrics by using an efficient and inexpensive new design for the nozzle-strip. Surface texture and physical properties of the hydroentangled fabrics produced using our new nozzle-strip were characterized and compared with those entangled using the traditional designs.

Waterjets and their impact forces

Efficient energy transfer in hydroentangling determines the degree of fiber entanglement. For an efficient energy transfer, it is important to have a high-quality waterjet, which has a long intact length (long breakup length) and stays collimated for the range of pressures used in hydroentangling, 30–400 bars (see Fig. 4). Such a jet is laminar and has a glassy appearance. To obtain a waterjet that stays laminar for the above pressure range, it is necessary to eliminate any wall-induced friction/vorticity that perturbs the water flow through the nozzle. This is only possible when the flow inside the nozzle is detached from the nozzle's inner walls, forming the so-called constricted waterjet (see Fig. 5). Such a detachment occurs when the flow is forced to make a sudden 90° turn while entering the nozzle. Note that non-constricted waterjets at the above pressure range will quickly turn into spray once they exit the nozzle, and their energy gets dispersed. Readers are referred to our previous works on constricted waterjets for detailed information [15–17; 8]. It is worth mentioning that the diameter of constricted waterjets, d_j is

$$d_j = \sqrt{C_d} d_n \tag{1}$$

where $C_d \cong 0.62$ is the discharge coefficient of sharp-edge capillary nozzles that generate constricted waterjets [15] and d_n is the nozzle inlet diameter. The most conventionally used nozzle inlet diameter, d_n, is 130 μm resulting in a waterjet of about 100 μm diameter (see Fig. 5). As mentioned above, hydroentangling waterjets have long breakup lengths. The diameter of the jets at the moment they impact the fiber-web, about 5 cm downstream, is almost the same as the diameter at the exit from the nozzles or $d_j = \sqrt{C_d} d_n$. The impact force, F, of a liquid jet is linearly proportional to its velocity, V, and flow rate, $\dot{m}$ for as long as it is not broken up into a spray.

$$F \propto \dot{m} V \tag{2}$$

where $\dot{m} = \frac{\pi}{4} \rho d_j^2 V$. Note that the velocity of a constricted jet can be calculated from its stagnation pressure via Bernoulli's equation, $V = \sqrt{2} p^{1/2} \rho^{-1/2}$, with sufficient accu-

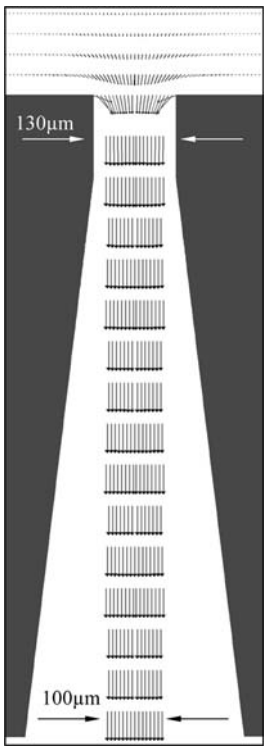

Fig. 5 Flow of a high-quality waterjet in a typical hydroentangling nozzle. It can be seen that the flow is detached from the nozzle's inner walls

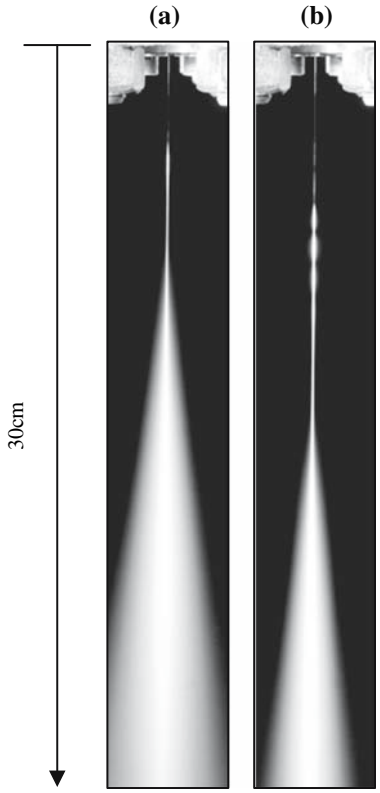

Fig. 6 Profile of two different waterjets issued from two nozzles having inlet diameters of 65 μm (**a**) and 130 μm (**b**) at a pressure of 100 bars

racy. Here p and ρ are the manifold's gauge pressure and the liquid's density, respectively. From Eq. 2, it can be seen that impact force of a waterjet is proportional to the square of its diameter. As will be discussed in section 'New concept for nozzle-strips', we plan to use this property of the jets to level the jet-streaks on the fabric's surface. In particular, we plan to impact the ridges in the jet-streaks with waterjets having smaller diameters (i.e., with lower impact forces). It, however, should be noted that reducing the diameter of the nozzle may result in the formation of waterjets with a shorter breakup length. As mentioned in section 'Introduction', the intact length of the jets should be at least 5 cm in order to reach the fabric before it breaks up. To examine the range of diameters that can be used to design a new jet-strip, a test setup was designed and built, which allows one to produce a single-waterjet, and image its profile [18]. This setup was used to examine the profiles of waterjets issued from different geometries at different pressures as well as their impact forces along their axis. Figure 6 shows the profile of two different waterjets issued from two similar nozzles having different inlet diameters of 65 μm and 130 μm at a pressure of 100 bars. It can be seen that the waterjet issued from the nozzle with 65 μm diameter has an apparent breakup length greater than 5 cm. This indicates that nozzle diameters greater than 65 μm will have sufficient intact length.

In order to measure the impact force of the above waterjets and compare our theoretical predictions via the momentum equation, i.e., Eq. 2, our experimental setup was equipped with a compression load cell, a load cell holder with an accurate height adjustment capability, and a data acquisition system controlled by a PC. The impact forces of these waterjets along their axes are measured and plotted in Fig. 7. Assuming a 90° deflection of the jet after the impact with a flat plate, we calculated the impact force of these waterjets and added them to Fig. 7 for comparison. As mentioned before, when a jet breaks up, its momentum is lost and its impact force is dispersed. Note that the results shown in Fig. 7 reveal a decline in the impact force of the jet from the nozzles with a diameter of 65 μm after at about 10 cm from the nozzle exit. Nevertheless, the impact force of this jet is still in agreement with Eq. 2 for the 1st 10 cm of its length (intact length).

It should be mentioned that the impact force of a waterjet with a fiber-web is numerically different from the above data obtained for a flat plate. However, the above proportionality between the impact force and nozzle diameter is still valid and these results can qualitatively be used to design a nozzle-strip. In the next section we describe a combination of nozzles with different diameters

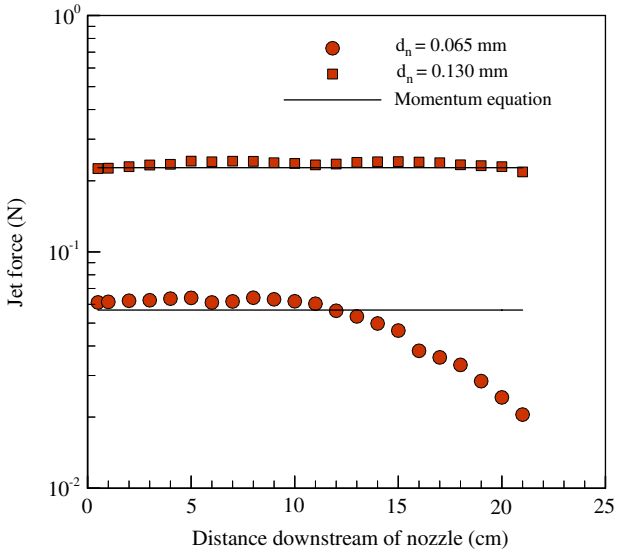

Fig. 7 Impact forces of waterjets issued from nozzles with 65 μm and 130 μm diameters at a pressure of 100 bars

and their role in minimizing the jet-streaks of the hydroentangled fabrics.

New concept for nozzle-strips

Typical hydroentangling nozzle-strips have a single row of nozzles with an inlet diameter of about 130 μm as shown in Fig. 8. The nozzle-to-nozzle spacing, s, is normally about 500–600 μm. While there have been attempts at developing multi-row strips, none employed nozzles with different inlet sizes as reported here. Our design is unique because of its simplicity and efficient performance which makes it attractive for the industry.

It is experimentally observed that the jet-streaks change every time the web is impacted by a waterjet curtain. Consequently, the jet-marks that permanently stay on the fabric are those which are caused by the last manifold. This is especially true when the last manifold operates at the highest pressure. The new nozzle-strip that we present in this paper is designed to be placed in the last manifold.

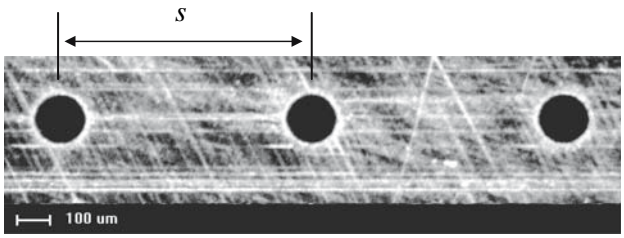

Fig. 8 Top view of a typical single-row nozzle-strip with an inlet diameter of 130 μm and a nozzle to nozzle distance of 600 μm

Figure 9 shows our design for the nozzle-strip. In this design, nozzles of two different diameters are arranged in two rows, in a staggered configuration. To minimize variations caused by the web structure, we designed a double-row nozzle-strip in which the 2nd row was segmented with each segment having a different diameter. The inlet diameter of the nozzles in the 1st row is kept constant at d_1 = 130 μm similar to the conventional nozzles (see Fig. 8) while the diameter of the nozzles in the 2nd row, d_2, are varied from 100 μm to 130 μm with an increment of 10 μm.

The above diameter range is chosen to ensure that the nozzles have acceptable breakup lengths, but have a lower impact force than the first row. The impact force of a waterjet discharged from a nozzle with 100 μm diameter is, for instance, 58% of that of a jet produced by a nozzle with 130 μm diameter.

Our reason for having a second row of nozzles (the row which the fabric passes through last), is based on the fact that the first row of waterjets (from the nozzles with 130 μm diameter) wash away the previously formed jet-marks, and create a final set of peaks and valleys. The waterjets in the 2nd row, being smaller in diameter and arranged in a staggered configuration, will impact the peak of the ridges formed by the first row (see Fig. 10) and would potentially alleviate the ridges without creating any new noticeable streaks.

Experiments

To examine the performance of our nozzle-strip, a spun-bonded web of Nylon/PET bicomponent fibers having

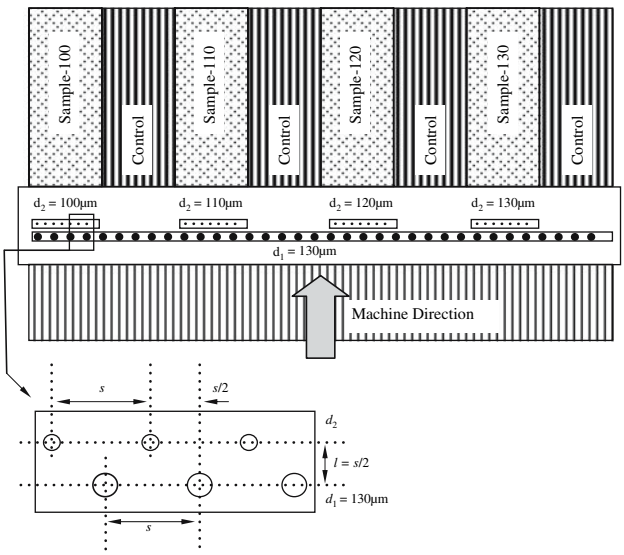

Fig. 9 The new nozzle-strip design having a continuous first row of nozzles with 130 μm diameter and segments of nozzles with different diameters in the second row

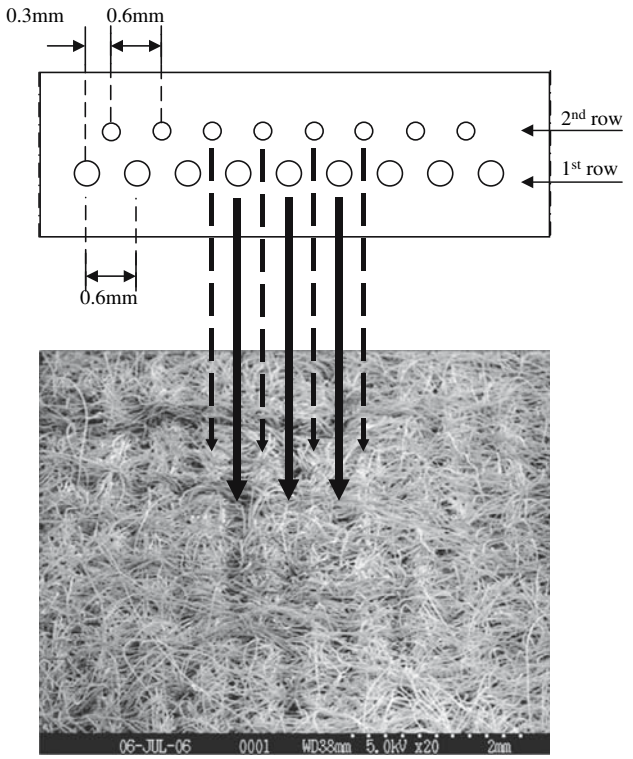

Fig. 10 Schematic of a double-row nozzle-strip with the arrows representing the waterjets of the first and second row impacting on the fabric's surface. Jets in the 1st row wash away the previous streaks and make new set of jet-streaks. The jets in the 2nd row hit the ridges and flatten them

an average diameter of 15 μm was prepared in the Partners' Nonwovens Laboratory at the Nonwovens Cooperative Research Center (NCRC), at North Carolina State University (NCSU). Spun-bonding is a manufacturing technique, which offers a one-step process for producing nonwovens from the raw materials (thermoplastic polymers) as the fiber and fabric production are combined. In spun-bonding, filaments are extruded from multiple banks of spinnerets [1]. These filaments are then drawn to their final diameters (about 15 micrometers) by two high-speed air-jets and laid down onto a porous substrate. These webs are usually thermally bonded by calender rolls. The basis weight, W_b, (defined as the mass per unit of area) of our fabric was 150 g/m^2. Our fabric was cold-calendered and therefore, the fibers were not thermally bonded, but were held together sufficiently to be unwound and hydroentangled.

Our new nozzle-strip was placed in the last manifold that the fabric would pass under (for example, manifold no. 3 in Fig. 2). The operating pressure considered for this manifold was 200 bars. The spun-bonded web was pre-entangled at a pressure of 150 bar using 4 manifolds (manifolds number 2–5 in Fig. 2) for 3 passes through the machine. It should be noted that manifold number 1 (see Fig. 2) is only used for ''pre-wetting'' the web for better entangling, and was run at an operating pressure of only 30 bars at all times. The operating pressure used for our experiment (where the Control fabric and Sample fabrics were compared) was 200 bars (in manifold number 3 in Fig. 2). For convenience, we refer to the fabric obtained from entangling using two rows of nozzles (within a segment) as ''Sample'', while the one obtained from entangling with a single row (between segments) is called ''Control'' (see Fig. 9). To distinguish between Samples treated with different nozzles, we add the nozzle diameter of the 2nd row to the above terminology.

Results and discussion

To compare the efficiency of different nozzle combinations in minimizing the jet-streaks, a texture analysis procedure was considered. The physical properties of the resulting fabric were also examined for completeness of the study. These results are reported in the following subsections.

Texture analysis

Figure 11a, b show two views of the Control and Sample-110 fabrics. Note the deep grooves (pointed by vectors) in the cross section of the Control fabric (Fig. 11a) with a spacing of about 600 μm, which are made by the waterjets and can reduce the mechanical strength of the fabric. Note that 600 μm is the spacing between the nozzles used in this study. Such non-uniformities are not detected in the cross section of Sample-110 as the fibers are better spread. 3D views of the Control and Sample-110 fabrics are shown in Fig. 11b. The reduction of jet-streaks in Sample-110 is evident.

To perform image analysis and numerically compare the Control and Samples, the fabrics were imaged using a high-resolution digital camera coupled with an optical microscope (see Fig. 12). The reduction in the jet-streaks is obviously visible to the naked eyes. In order to examine the extent to which jet-streaks are eliminated, five different areas of each specimen were imaged, and analyzed using the co-occurrence method [19–23]. The fabrics were illuminated using macro-dark field illumination for better visibility. Spatial co-occurrence analysis was performed to evaluate the jet-streaks' periodicity [23]. Prior to performing the co-occurrence analysis, the images were converted to grayscale, and a central portion with a size of 400 pixel × 400 pixel was chosen for the analysis. The processed images (binary) are placed next to the images of each specimen (Fig. 12) for comparison. For more infor-

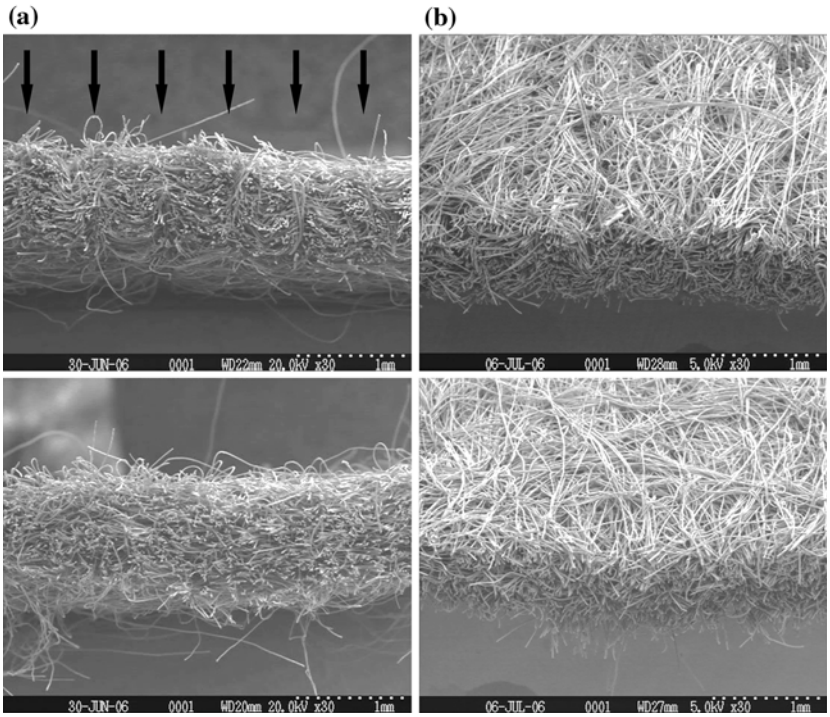

Fig. 11 SEM images of (**a**) cross-sectional and (**b**) isometric views of Control and Sample-110. Vectors represent the waterjets with a spacing of 600 μm

mation about the details of this analysis, the readers are referred to the work of Shim and Pourdeyhimi [23].

The co-occurrence analysis (see Fig. 13a) reveals the presence of dominant peaks occurring at a period of about 600 μm for the jet-streaks in the Control fabric. The results obtained from the Sample fabrics show different amplitudes indicating that the jet-streaks are reduced. It can be seen that the Sample-110 has the best performance for the pressures considered in this experiment. The power values shown in Fig. 13b represent the intensity of the jet-streaks in a fabric. The obtained curves represent the periodicity of the jet-streaks in the fabrics (occurring every 600 μm), and the height of each curve indicates its dominance. In other words, power is representative of the amplitude obtained from the contrast curves. Obviously, the new nozzle-strip design has decreased the intensity of the jet-streaks defect.

Tear test

As mentioned earlier, presence of the jet-streaks on the fabric can weaken the tear resistance of the fabric. The SEM images of the fabric's cross-section (Fig. 11a, b) clearly show that the thickness of the fabric is locally reduced in the jet-streaks as the fibers are pushed away from these areas. These grooves can cause stress concentration and therefore, decrease the tear resistance of the fabric in the machine direction. To examine the effect of our new nozzle-strip in improving the fabric's strength, we tested our Samples' tear resistance in the machine direction and compared them with that of the Control fabric. The tear test considered here measures the force required to tear a specimen in which the tear is initiated before testing. According to ASTM D2261–96 ''Standard Test Method for Tearing Strength of Fabrics by the Tongue (Single Rip) Procedure (Constant-Rate-of-Extension Tensile Testing Machine)'' a rectangular specimen (75 mm × 200 mm) is precut in the center of the long edge to form a two-tongued or trouser shaped specimen. One tongue is clamped into the lower jaw of the machine and the other is clamped into the upper jaw. During the measurement, the distance between the jaws increases and the force applied to the fabric, due to the movement of the jaws, propagates the tear. Figure 14 shows two specimen representing the rupture propagation in the Control and Sample-110 fabrics. It can be seen that the rupture perfectly propagates along the jet-streaks in the case of Control fabric. The tear propagation shown in Fig. 14 is a typical behavior observed in most of the tested specimen. This is because the jet-streaks have made areas of minimum resistance which are perfectly aligned in the machine direction. The rupture-front in the case of Sample-110, however, did not reveal presence of straight lines of defects. Tear in this case tends to follow a path of minimum resistance which is not necessarily in the machine direction.

During the tear test, the force required to move the clamps is reported. Figure 15 shows the force-strain curves obtained from conducting the tear test on 5 replicates of the Control and Sample-110 fabrics. The results are normal-

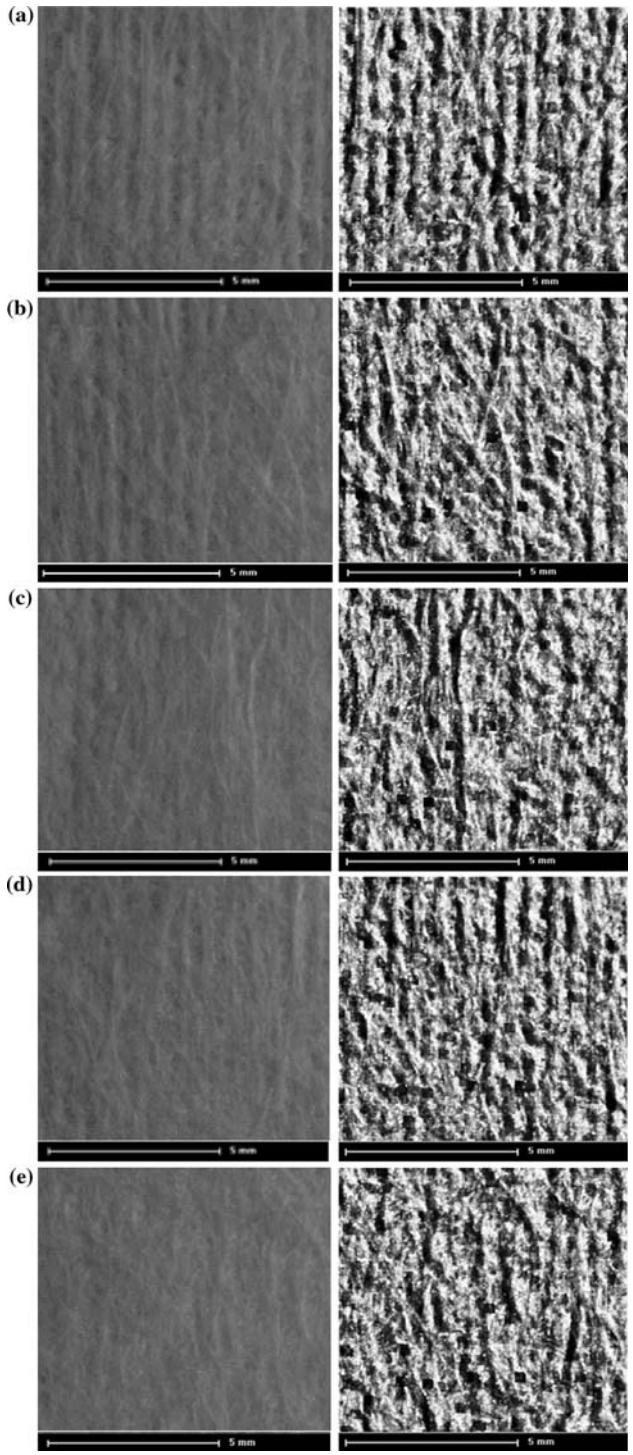

Fig. 12 Microscopic images of the Control fabric (**a**), Sample-100 (**b**), Sample-110 (**c**), Sample-120 (**d**), and Sample-130 (**e**) along with their processed (binary) counterparts

ized with the average resistance of the Control fabric for better comparison. An improvement of about 30% in the tear resistance of the fabric is evident. Similar tests have also been performed on Sample-100, Sample-120, and

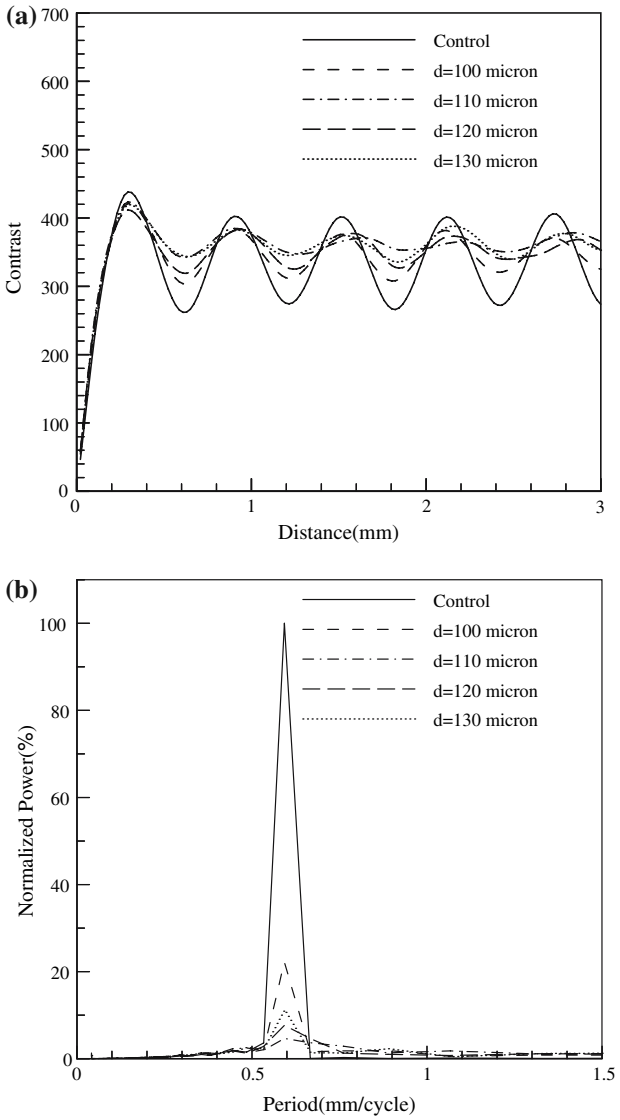

Fig. 13 Co-occurrence curves (**a**) and periodicity curves (**b**) of the Control and Sample-100, Sample-110, Sample-120, and Sample-130. The power values are normalized with that of the Control fabric

Sample-130. These results, in agreement with the results of the co-occurrence experiment, revealed that Sample-110 has the most uniform surface and so the highest tear resistance. The load values increase rapidly with the strain and reach a plateau after an elongation of about 100% where they start fluctuating until the specimen is completely ruptured. The initial increase in the load is the force needed to bring the fabric under tension without the rupture-front moving. The tear resistance is averaged from the point where the rupture-front starts moving towards the end of the specimen, i.e., at about 100% elongation, up to the point where the failure occurs. The average normalized tear resistances of the Samples and their corresponding standard deviations are shown in Table 1.

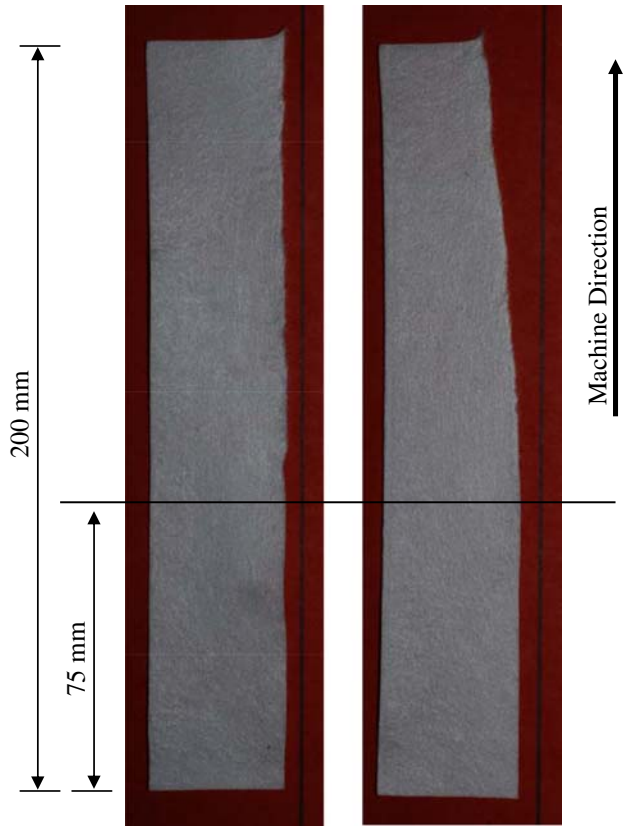

Fig. 14 Images of the Control and Sample-110 after tear test in the machine direction. One half of each specimen is shown. Note that the rupture has perfectly progressed along the jet-streaks (machine direction) in the case of the Control fabric (picture to the left). The rupture has deviated from the machine direction in the case of the Sample-110 indicating the lack of a perfect path of minimum resistance along the machine direction

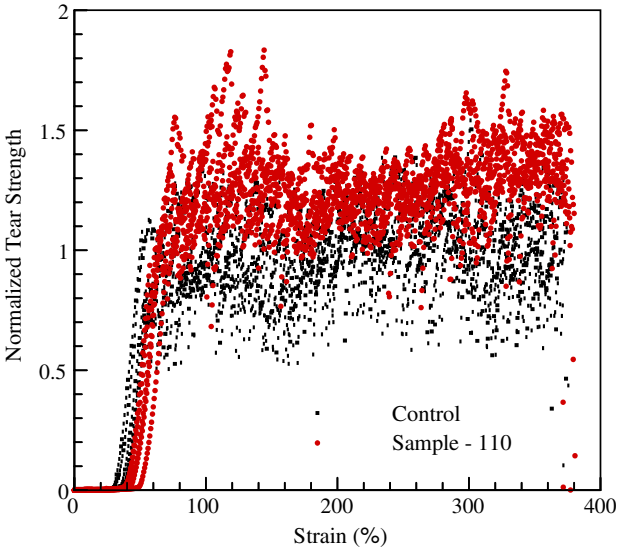

Fig. 15 Normalized tear strength results versus strain for five replications of the Control and Sample-110. The data are normalized with the average tear resistance of the Control fabric for better comparison

Table 1 Normalized mean tear resistances of the samples together with their standard deviations

	Sample-100	Sample-110	Sample-120	Sample-130
Normalized average tear strength	1.11	1.30	1.28	1.20
Standard deviation	0.02	0.03	0.01	0.03

Tensile tests

One of the most invaluable properties of hydroentangled fabrics is their tensile strength. It is important to ensure that improving the tear resistance of the fabrics does not affect their tensile strength. For this reason, all the fabrics treated with our new strip were examined according to the ASTM D 5035–95 entitled ''Standard Test Method for Breaking Force and Elongation of Textile Fabrics (Strip Method)''. This test reports the force required to break a textile specimen in the tensile direction. According to this test, a rectangular specimen (25 mm × 150 mm) is mounted on the upper and lower jaws of the tensile testing machine with its longer dimension parallel to the direction of force application. The distance between the jaws is increased until the failure occurs. The force required to break the textile specimen and the elongation of the specimen are reported during the measurement.

Figure 16 shows the force-strain curves obtained from conducting the above test on 5 replicates of the Control and Sample-110 fabrics. These results are normalized with the maximum average tensile strength of the Control fabric (at rupture) for better comparison. Figure 16 reveals that there is no remarkable change in the tensile properties of Sample-110 in the machine direction. The normalized average tensile strengths of the Sample-100, Sample-120, and Sample-130 are shown in Table 2 for comparison. It is evident that none of the Sample fabrics show any reduction in their tensile properties.

Conclusions

The jet-streaks caused by the hydroentangling process are undesirable and degrade the properties of the fabrics produced by hydroentangling. In this paper, we reported a new nozzle-strip design for minimizing the jet-streaks. In particular, we demonstrated that a waterjet curtain made up of two rows of staggered jets with the jets in the 2nd row being smaller in diameter than those in the 1st row can help minimizing the jet-streaks. The optimal ratio between the diameter of the jets in the 1st and 2nd row depends on the

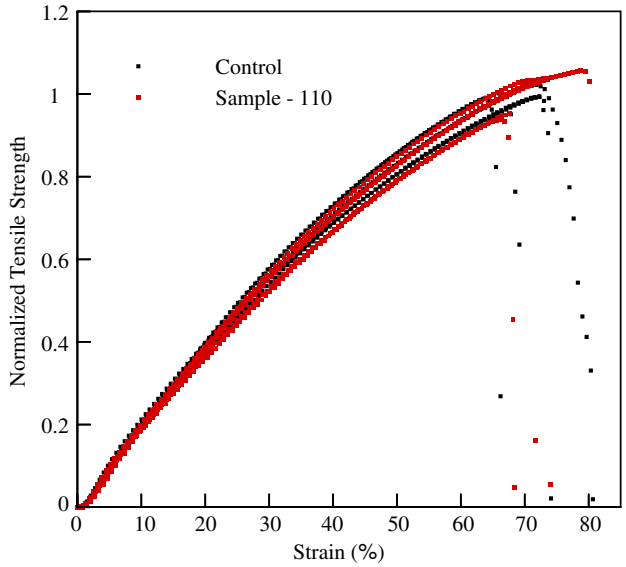

Fig. 16 Normalized tensile strength results versus strain for five replications of the Control and Sample-110. The results are normalized using the average maximum tensile resistance of the Control fabrics for better comparison

Table 2 Normalized mean tensile strengths of the samples together with their standard deviations

	Sample-100	Sample-110	Sample-120	Sample-130
Normalized average tensile strength	1.09	1.01	0.98	1.01
Standard deviation	0.06	0.05	0.03	0.02

hydroentangling pressure, as well as web characteristics. For the fiber-web and operating pressures considered in this work, a combination of nozzles with a diameter of 130 μm in the 1st row, and nozzles with a diameter of 110 μm in the 2nd row, was found to be the optimum setting for minimizing the jet-marks in hydroentangled fabrics. Our results also indicate that using the new nozzle-strip, the fabric's tear strength was improved by about 30% while the tensile strength remained unaffected.

Acknowledgements The current work is supported by the Nonwovens Cooperative Research Center (NCRC). Nippon Nozzles and Groz-Beckert are acknowledged for manufacturing our hydroentangling nozzle-strips.

References

1. Butler I (1999) In: The Nonwoven Fabrics Handbook. Association of the Nonwoven Fabrics Industry—INDA, Cary, NC
2. White CF (1990) Tappi J 73(6):187
3. Connolly TJ, Parent LR (1993) Tappi J 76(8):135
4. Acar M, Harper JF (2000) Comput Struct 76(1–3):105
5. Ghassemieh E, Acar M, Versteeg HK (2001) Compos Sci Technol 61:1681
6. Ghassemieh E, Acar M, Versteeg HK (2002) J Mater: Design Appl 216(L3):199
7. Ghassemieh E, Acar M, Versteeg HK (2002) J Mater: Design Appl 216(L4):211
8. Anantharamaiah N, Vahedi Tafreshi H, Pourdeyhimi B (2006) Chem Eng Res Des 84(A3):231
9. Anantharamaiah N, Vahedi Tafreshi H, Pourdeyhimi B (2006) Exp Fluids 41(1):103
10. Fleissner G (2000) US Patent 6105222
11. Kobayashi T, Ishikawa H (2003) US Patent 6571441
12. Oathout JM, Staples PO, Miller DF (2005) US Patent 6877196
13. Zolin PF (2001) US Patent 6253429
14. Greenway JM, Lawrence J, Sternlieb H, Ty F, Malaney FE (2003) US Patent 6557223
15. Vahedi Tafreshi H, Pourdeyhimi B (2003) Exp Fluids 35:364
16. Vahedi Tafreshi H, Pourdeyhimi B (2004) Text Res J 74(4):359
17. Anantharamaiah N, Vahedi Tafreshi H, Pourdeyhimi B (2006) Chem Eng Sci 61:4582
18. Begenir A, Vahedi Tafreshi H, Pourdeyhimi B (2004) Text Res J 74(2):178
19. Sobus J, Pourdeyhimi B, Gerde J, Ulcay Y (1991) Text Res J 61(10):557
20. Sobus J, Pourdeyhimi B, Xu B, Ulcay Y (1992) Text Res J 62(1):26
21. Pourdeyhimi B, Sobus J, Xu B (1993) Text Res J 63(9):523
22. Pourdeyhimi B, Xu B, Wehrle L (1994) Text Res J 64(1):21
23. Shim E, Pourdeyhimi B (2005) Text Res J 75(7):569